RBGF
ISSN:1984-2295
Revista Brasileira de Geografia Física
Homepage: https://periodicos.ufpe.br/revistas/rbgfe
REVISTA BRASILEIRA DE GEOGRAFIA FÍSICA

Effect of climate change on water flow and sediment flow

Eder Alexandre Schatz Sá[1], Ildelgardis Bertol[2], Silvio Luís Rafaelli Neto[3], Claudia Guimarães Camargo Campos[4], Carolina Natel de Moura[5], Paula Carvalho da Silveira[6]

[1] Dr. em Ciências do Solo, Professor, Centro de Ciências Agroveterinárias, Universidade do Estado de Santa Catarina, Av. Luiz de Camões, 2090, CEP 88520-000, Lages, Santa Catarina. eder.sa@udesc.br (autor correspondente). [2] Dr. em Ciências do Solo, Professor, Centro de Ciências Agroveterinárias, Universidade do Estado de Santa Catarina, Av. Luiz de Camões, 2090, CEP 88520-000, Lages, Santa Catarina. ildegardis.bertol@udesc.br. [3] Dr. em Engenharia, Professor, Centro de Ciências Agroveterinárias, Universidade do Estado de Santa Catarina, Av. Luiz de Camões, 2090, CEP 88520-000, Lages, Santa Catarina. silvio.rafaeli@udesc.br. [4] Dr. em Meteorologia, Professora, Centro de Ciências Agroveterinárias, Universidade do Estado de Santa Catarina, Av. Luiz de Camões, 2090, CEP 88520-000, Lages, Santa Catarina. claudia.campos@udesc.br; [5] Dr. em Engenharia de Recursos hídricos, Centro de Ciências Agroveterinárias, Universidade do Estado de Santa Catarina, Av. Luiz de Camões, 2090, CEP 88520-000, Lages, Santa Catarina. carolina.natel@hotmail.com. [6] Engenheira ambiental e Sanitarista, Centro de Ciências Agroveterinárias, Universidade do Estado de Santa Catarina, Av. Luiz de Camões, 2090, CEP 88520-000, Lages, Santa Catarina. paulaa_silveira@hotmail.com.

Artigo recebido em 30/10/2023 e aceito em 10/09/2024

A B S T R A C T
This work was based on the hypothesis that in climate change scenarios, the hydrosedimentological cycle is affected and the amount of sediment produced in the basin is altered. The area used for the study is the Marombas river watershed, located in the mountainous region of the Santa Catarina state. The projection of future flow was carried out by the Soil and Water Assessment Tool (SWAT) model, under the climate scenarios RCP 4.5 and RCP 8.5, in the period between 2020 and 2099. The SWAT model was calibrated on a daily scale between 1979 and 1989 years and validated between 1994 and 1997 years. The Nash-Sutcliffe values found were 0.91 for calibration and 0.74 for flow validation and 0.74 for calibration and 0.50 for sediment validation. The hydrological projection for the period 2020-2099 indicated an increase in the average monthly flow of 10% and 17% for the RCP 4.5 and RCP 8.5 scenarios, respectively. There was a 40% increase in the modal flow (Q50) in both scenarios evaluated, in addition to extreme events in RCP 8.5. The grantable flow reduced 11% to Q95 in both scenarios, and 26% and 27% to Q98 in the RCP 4.5 and RCP 8.5 scenarios, respectively. There was also a tendency for sediment production to be up to three times higher, attributed to the better temporal distribution of rainfall that increased soil moisture and favored the increase in flow and water erosion.
Keywords: Eta-HadGEM2-ES, Hydrological modeling, SWAT.

Efeito das mudanças climáticas na vazão e no fluxo de sedimentos

R E S U M O
Esse trabalho se baseou na hipótese de que em cenários de mudança climática, o ciclo hidrosedimentológico é afetado e a quantidade de sedimentos produzidos na bacia é alterada. A área utilizada para o estudo é a bacia hidrográfica do Marombas, localizada na região serrana do estado de Santa Catarina. A projeção da vazão futura foi realizada pelo modelo Soil and Water Assessment Tool (SWAT), sob os cenários climáticos RCP 4.5 e RCP 8.5, no período dentre 2020 a 2099. O modelo SWAT foi calibrado em escala diária entre os anos de 1979 e 1989 e validado entre 1994 e 1997. Os valores de Nash-sutcliffe encontrados foram de 0,91 para a calibração e 0,74 para validação de vazão e de 0,74 para a calibração e 0,50 para a validação de sedimentos. A projeção hidrológica para o período 2020-2099 indicou aumento da vazão média mensal de 10 % e 17 % para os cenários RCP 4.5 e RCP 8.5, respectivamente. Houve um aumento de 40% na vazão modal (Q50) nos dois cenários avaliados, além de eventos extremos no RCP 8.5. A vazão outorgável reduziu 11% para Q95 em ambos os cenários, e 26% e 27% para Q98 nos cenários RCP 4.5 e RCP 8.5, respectivamente. Também, houve tendência de produção de sedimentos até três vezes maior, atribuída à melhor distribuição temporal das chuvas que elevou a umidade do solo e favoreceu o aumento da vazão e da erosão hídrica.
Keywords: Eta-HadGEM2-ES, Modelagem hidrológica, SWAT.

Introduction

The distribution of rainfall varies in time and space, due to the fact that the meteorological elements that characterize it change temporally and spatially, due to changes in the behavior of the parameters that condition it. This variability is constantly related to the term climate change (Seebocus et al., 2021). According to the Intergovernmental Panel on Climate Change -

IPCC (2007), climate change is defined as changes in the climate over time due to natural variability and/or the result of human activities.

According to Barry and Chorley (2013), the temporal variability of the climate caused by a natural process is mainly due to external forces, such as the variation in the intensity of solar radiation that reaches the top of the atmosphere due to oscillations in the solar cycles, and due to the internal forces of the lithosphere such as the eruption of volcanoes. Anthropic activity, in turn, is often related to the intensification of this climatic variability. This started to happen mainly after the industrial revolution in which the continuous development of society occurred with an intense use of fossil fuels. Its speed and intensity is greater and, for this reason, it has been the object of concern of the world scientific and political community (Koehler et al., 2002).

Several studies indicate that fossil fuels, mainly carbon dioxide (CO2), are the main causes of the increase in the concentration of greenhouse gases 120 (GHGs) in the Earth's atmosphere. Data from the IPCC report (1970) already indicated a continuous increase in the concentration of CO2 and methane gas (CH4). A study also produced by the IPCC (2013) indicated an increase of 40% and 150% in the concentration of CO2 and CH4, respectively. Researchers from the Integrated Carbon Observation System (ICOS) also observed an increase in the concentration of CO2 in the atmosphere, from 227 ppm in 1975 to 403 ppm in 2016 (Le Quéré et al., 2015). Other sources of CO2 are deforestation, burning and extensive livestock farming (Koehler et al., 2002).

According to Filonchyk et al. (2024), a series of studies indicate that this increase in the concentration of GHGs is one of the main causes of current climate change, attributing the increase in the planet's average temperature to the accumulation of these gases in the atmosphere.

In this line of research, the increase in the concentration of GHGs causes a greater amount of long-wave solar radiation to remain close to the surface, causing changes in the planet's energy balance. In addition to GHGs, there are anthropic factors that increase climate change: urbanization without adequate land use planning (Zhenmei et al., 2008) and forest degradation (Groppo et al., 2005).

In recent decades, the IPCC has focused part of its studies on projecting future scenarios of rising air temperatures resulting from this climate change. In the most recent IPCC reports (2023), it was found that global temperatures have already risen by approximately 1.1ºC compared to pre-industrial levels (1850–1900). If greenhouse gas emissions continue at the current pace, temperatures could increase by 3.3ºC to 5.7ºC by 2100, depending on the scenario. Additionally, it is highly likely that a 1.5ºC increase will be reached or exceeded between 2021 and 2040 in most analyzed scenarios.

Climate deregulation also affects other meteorological elements, such as air humidity, wind speed (Breslow & Sailor, 2002; Harrison et al., 2008; Shui et. al., 2024), precipitation, and all physical, chemical and biological processes. The change in the rainfall regime, for example, affects all process of the hydrological cycle, reflected in drought and flood events that vary in frequency and scale (Mazurczyk et al., 2018). Other climate and surface changes that have been constantly attributed to climate change are: the melting of polar ice caps (Poelking et al., 2014; Moser et al., 2024), heat waves (Schär et al., 2004; Bitencourt et al., 2020), annual water deficits (Ciais et al., 2005; Lovino et al., 2020) andrising sea levels (Marengo, 2006; Mckay et al., 2011; Filgueras et al., 2024).

Given these results, a series of climate variables have been studied in various regions of the world in recent years, with the aim of testing the hypothesis that there is a change in climate behavior (De Moura, 2018) and that this change affects populations differently across the planet. In Brazil, for example, the National Institute of Science and Technology for Climate Change (INCT for Climate Change) was created in 2008, composed of a number of universities that collaborate on research to provide a sufficient scientific basis for understanding global environmental changes and their impacts, studying adaptation measures and reducing the population's vulnerability to these changes, and promoting mitigation techniques and the development of technological products.

The results of studies on climate change impacts on rainfall, for example, have indicated significant spatial variability in these changes. While in some areas rainfall volume tends to increase considerably, in others droughts are becoming more frequent. In southern Brazil, for instance, studies such as those by Groissman et al. (2005) and Salviano et al. (2016) have identified a trend of increasing precipitation volume and extreme rainfall events. This highlights the clear need for regional studies on how climate change may unfold, aiming to gather local and regional information that can support future planning and decision-making.

The increase in rainfall volume also affects the amount of water to be transported via surface runoff. The increase in surface runoff enhances the disaggregation and transport of soil particles, increasing water erosion. In addition to rainfall, other factors affecting the erosion process should be considered, such as evapotranspiration, the leaf area index (LAI) which affects vegetation interception, microbial activity in the soil, etc. All these factors contribute to climate change, whether caused by anthropogenic factors or not, affecting soil erosion.

Water erosion is considered the most intense and comprehensive form of soil degradation, because cause reducing the productive capacity of the soil, in addition to serious environmental damage such as siltation and pollution of water courses (Wang et al., 2014, Kalkhoff et al., 2016). Rain is the agent responsible for the energy necessary for the occurrence of water erosion, both in the stage of disintegration, transport and deposition soil particles (Amore et al., 2004).

Currently, few studies have been conducted to evaluate the behavior of erosion in relation to climate change, which is also responsible for altering the intensity and frequency of the erosion process. The work of Lelis et al. (2011) stands out as one of the few studies on the topic in Brazil, which, using the IPCC A1B scenario, considered the most pessimistic, found a soil loss and runoff rate much higher than current levels, reaching up to three times higher in a critical situation of increased precipitated volume and with the occurrence of rainfall peaks. Another study by Lensen et al. (2015) simulated the impacts of climate change on the Apucaraninha River basin (504 km²) in southern Brazil, using the A2 (pessimistic) and B2 (optimistic) scenarios from the IPCC. The results indicated that each 1% increase in precipitation resulted in a 2.8% increase in erosion and a 1.6% increase in runoff in the A2 scenario, and a 2.3% increase in erosion and a 1.1% increase in runoff in the B2 scenario, suggesting that climate changes have a greater impact on sediment production.

Elsewhere in the world, other studies have been carried out, such as the study conducted in the central region of India, in the Betwa River basin (Pandey & Palmare, 2019), which also observed an increase in erosion severity in the future due to changes in precipitation. However, the results indicated much smaller increases, ranging from 1 to 2% in the severe and very high erosion classes. Another more recent study, conducted by Escobar and Carvalho-Santos (2022) in Portugal, indicated that average sediment export would increase by 76% under the RCP 8.5 scenario, corroborating the high values found by Lelis et al. (2011).

This work was based on the hypothesis that climate changes alter the mechanism of water erosion, influencing the amount of material carried via runoff to the lower areas of the relief, as they influence the intensity and volume of rain. In theory, an increase in runoff resulting from an increase in the volume and intensity of rainfall, favors the desagregation and transport of soil particles, intensifying the water erosion process. This climatic factor assumes an even greater weight in soil losses in tropical regions, where the variation of air and rain temperature controls, in a more intense way, the magnitude of the erosion process (Machado et al., 2008; Zou et al., 2024).

This lack of studies on the topic and the discrepancy in the results found in the estimates of future flow based on the climate change scenario justifies the realization of this study, considering the large contribution area of the Marombas Hydrographic Basin (MHB), located in the highlands of Santa Catarina, Brazil, and its importance from an agricultural and water resource management point of view. Thus, the objective of this study was to evaluate the effect of changes in rainfall patterns, resulting from climate change, on the flow of sediments at the hydrographic basin level.

Materials and Methods

Study Area

The study was carried out in the Marombas hydrographic basin (MHB), belonging to the Canoas river hydrographic basin, located between the geographical coordinates 26º45'20” and 27º21'00” of south latitude and between 51º02'10” and 50º10'35” of west longitude in the mountainous region of the state of Santa Catarina (Figure 1). It is an important area for the management of water resources in the south of Brazil, as it comprises several springs and tributaries of the Canoas River, considered one of the main recharging regions of the Guarani Aquifer.

According to the Köppen classification, the region's climate is “Cfb”, mesothermal, humid subtropical, with cool summers and with well-distributed rain throughout the year. The average annual air temperature is 13.4 ºC to 16.4 °C, with an average annual precipitation of 1650 mm, with a maximum and minimum of 2500 and 1082 mm, respectively and average annual relative humidity between 71% and 83%.

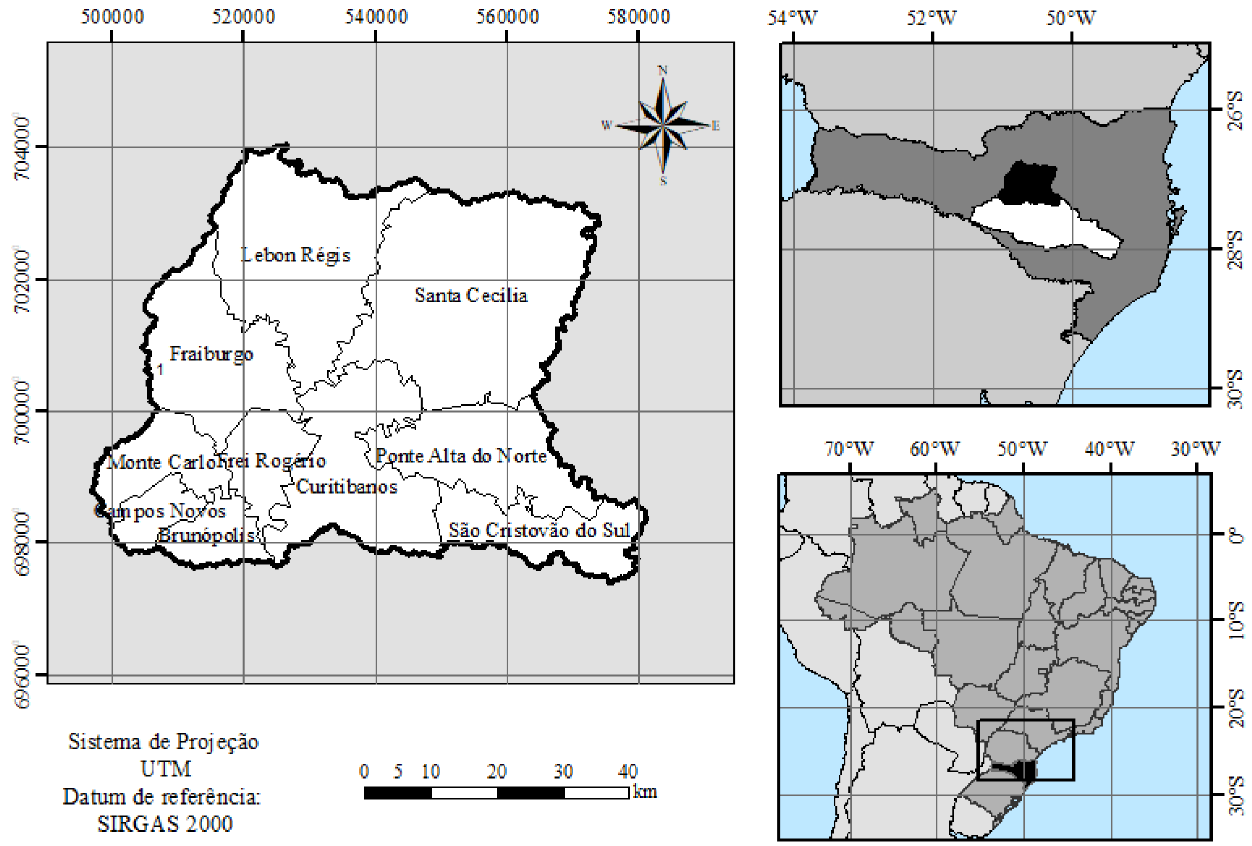

Figure 1. BHM location map.Source: Author (2023).

Variáveis Ambientais

Land use in MHB at the time used for the study was predominantly composed of fields (42%) and native forest (39%), and the main types of soil in the study region are Nitossolo Bruno (55%) and Cambissolo Húmico (28%) (EPAGRI, 2004). In addition to the aforementioned types of soil, the area still has sites with Neosolo Litolico (13%), Latossolo Bruno (3%) and small plots of Gleissolo Háplico and Organossolo Mésico. With regard to orography, flat to soft wavy relief (0-8%) and wavy relief (8-20%) predominate, according to the EMBRAPA classification (1979).

Entry Data

The rain data for the execution of the study were obtained from the rainfall stations of Passo Marombas, Ponte do Rio Antinhas, Ponte Alta do Norte and Lebon Régis and the flow data of the river fluviometric station of Passo Marombas, located in the basin of the study watershed. The data necessary for the calculation of potential evapotranspiration (PET) by Penman-Monteith were obtained from daily data from the Lages/SC weather station of EPAGRI/CIRAM/INMET (27°08' south latitude and 50°34' west longitude).

The historical series of observed sediments was obtained from the flow-sediment curve at the Passo Marombas fluviometric station (Geological Survey of Brazil CPRM), which has data on point measurements of suspended sediment concentration. 84 measurements were used, carried out between the years 1978 to 2017. The sediment concentration data in suspension were converted into mass flow from the equation:

$$F = 86{,}4 \times Q \times CSS \qquad (1)$$

where, F is the mass flow in the section (kg day-1), Q is the flow (m³ s-1) and CSS is the concentration of suspended solids (mg L-1).

The mass flow data were correlated with the flow data in order to obtain the regression equation used to construct the series of estimated sediment data. Two regression equations were defined. The first was obtained based on data from 1978 to 2017 and was used for calibration and the second obtained based on data from 1993 to 2017, and was used for model validation.

Climatic data for maximum and minimum air temperature, relative humidity, wind speed, solar radiation, and rainfall were obtained from the regionalized ETA-HADGEM2-ES model, with a resolution of 20 km. Two future greenhouse gas emission scenarios were considered: RCP 4.5 and RCP 8.5. For validation, the period from 1961 to 1990, corresponding to the climatological normal, was used, and for the projection of flow and sediment production, the period from 2020 to 2099. The data were provided by the National Institute for Space Research (INPE), in partnership with the State University of Santa Catarina (UDESC).

Experimental Design

The experiment initially consisted of calibrating and validating the Soil and Water Assessment Tool (SWAT) hydrological model for the flow and sediment flow in the Passo Marombas hydrographic basin. From the calibrated model, climate projection data, derived from the freely accessible ETA-HADGEM2-ES climate model in the RCP 4.5 and RCP 8.5 scenarios, were inserted into the hydrological model in order to evaluate the differences found between the current scenarios and the projected climate scenarios (Figure 2).

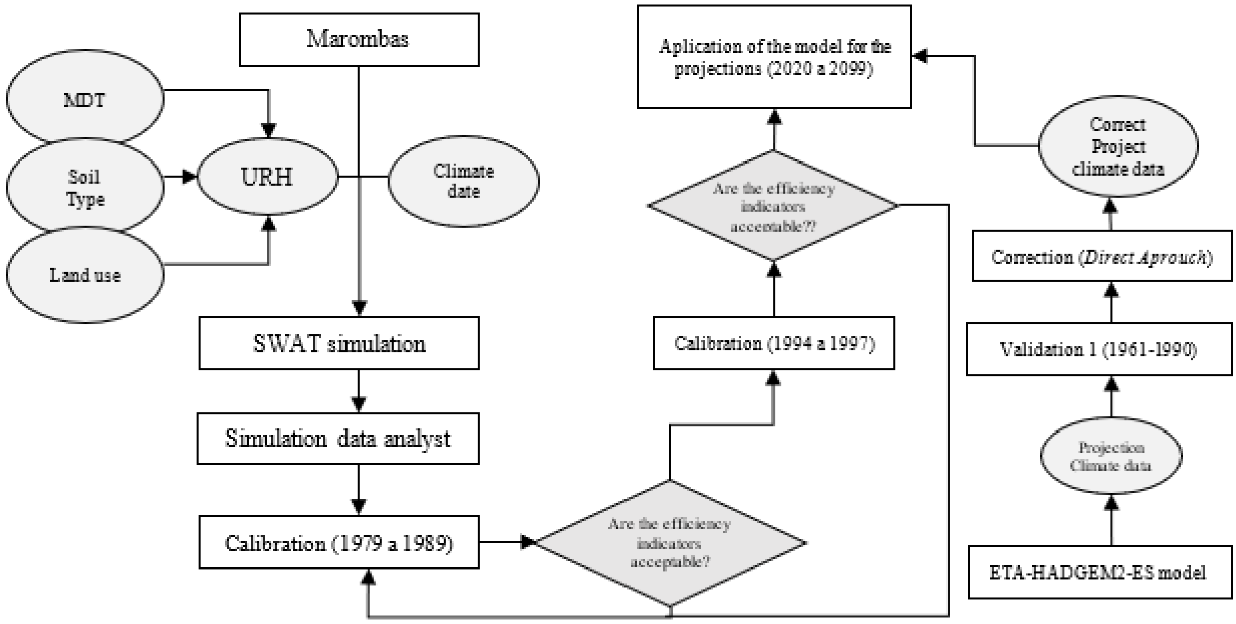

Flowchart of the calibration and validation steps of the SWAT model. Source: Author (2023).

Calibration and Validation of the Hydrological Model

The hydrological model used was the SWAT, developed in the 1990s, in the United States, by the Agricultural Research Service and Texas A & M University. The SWAT model is semi-distributed and continuous over time, developed to simulate the impact of land use change in medium and large hydrographic basins (Arnold et al., 2012; Tan et al., 2020). The model was calibrated and validated at the Passo Marombas fluviometric station for the variables average daily flow and sediment production. For the calibration and validation of the model, the SWAT-CUP software was used and the SUFI-2 was used as an uncertainty analysis method. We opted to use the SUFI-2 method because it allows a small number of executions to achieve a good range of forecasting uncertainties (Yang et al., 2008).

The model was calibrated on a daily scale for eleven years, between 1979 and 1989, with a warm-up period of two years (1977 and 1978), in order to characterize the previous moisture conditions of the soil. The validation period comprises the years 1994 and 1997, with the use of the year 1993 as heating. The choice of parameters used for the calibration of the model was based on the literature review and on the sensitivity analysis of the parameters. The references used include Sartori (2005), Baldisserra (2005), Embrapa (2015), and Antunes (2015).

The objective-function used to measure the model's accuracy was the Nash and Sutcliffe index (NSE) according to the following equation:

$$NSE = 1 - \frac{\sum_{i=1}^{n}(O_i - S_i)^2}{\sum_{i=1}^{n}(O_i - \bar{O})^2} \quad (2)$$

where, n is the observation time period (day); O_i is the observed flow of the ith day ($m^3\ s^{-1}$); S_i is the simulated flow for the ith day ($m^3\ s^{-1}$); $\bar{O}$ is the average flow observed i in the period ($m^3\ s^{-1}$); $\bar{S}$ is the average flow simulated in period i ($m^3\ s^{-1}$).

Validation of ETA-HADGEM2-ES Model Data.

The climatic data from the ETA-HADGEM2-ES model were submitted to validation before entering the SWAT model. The validation of the climate model ETA-HADGEM2-ES was carried out by comparing the climate data projected by the model and the historical series of data observed in the weather station for the period from 1961 to 1990, here called the control period. For the validation of the projected climatic data (maximum temperature, minimum temperature, relative humidity, wind speed and solar radiation), data from the meteorological station in Lages compared to the data extracted from the grid point of the model ETA-HADGEM2-ES which is in the same location as the station.

The validation of the rain data was based on the comparison of the data observed in the rain stations used in the calibration of the model with the estimated data extracted from the grid points of the ETA-HADGEM2-ES model closest to the respective station. The location of the rain gauges and the grid points corresponding to them can be seen in Figure 3 period ($m^3\ s^{-1}$); $\bar{S}$ is the average flow simulated in period i ($m^3\ s^{-1}$).

The validation was performed based on the monthly values of the variables since the model uncertainties related to the daily data are very high. The data of monthly averages simulated by the climate model and observed at the weather station were subjected to the correction of systematic errors using the direct aprouch method, whenever there was a significant difference according to the t Test. This methodology is consistent with the approach used by Moura (2020).

The climatic data of maximum and minimum air temperature, wind speed, relative humidity and solar radiation were corrected based on Equation 3 and rainfall data were corrected based on Equation 4 following the methodology proposed by Oliveira et al. (2015).

$$Cz_{corr_{i,j,k}} = Cz_{sim_{i,j,k}} \times [Cz_{obs_k}(61-90) - Cz_{sim_k}(61-90)] \quad (3)$$

where, $Cz_{corr_{i,j,k}}$ is the value of the climate variable z corrected for the evaluation period, on day i, in month k, in year j; $Cz_{sim_{i,j,k}}$ is the value of the same climate variable simulated in the same period, day, month, year; Cz_{obs_k} (61-90) is the observed mean of the climate variable z, in the control period, in month k; Cz_{sim_k} (61-90) is the simulated average of the climate variable z, in the control period, in month k.

While Equation 4 is expressed by:

$$P_{corr_{i,j,k}} = P_{sim_{i,j,k}} \times \frac{P_{obs_k}(61-90)}{P_{sim_k}(61-90)} \quad (4)$$

where, $P_{corr_{i,j,k}}$ is the corrected rainfall value for the evaluation period, on day i, in month k, in year j; $P_{sim_{i,j,k}}$ is the value of the same climate variable simulated in the same period, day, month, year; P_{obs_k}(61-90) is the observed average rainfall, in the control period, in month k; P_{sim_k}(61-90) is the simulated average rainfall, in the control period, in month k.

The normality and similarity of the variances of the simulated and observed data was tested using Shapiro-Wilk (Royston, 1982) and Levene (Fox, 2008), respectively. The t-test of independent samples was used to compare monthly averages of the variables air temperature (minimum and maximum), relative humidity, solar radiation, wind speed and rain at a significance level of 0.05.

MHB Flow and Sediment Flow Projections

The climatic data projected by the corrected ETA-HADGEM2-ES model were inserted in the model for the projections of the average monthly flow and sediment flow. The sediment flow and flow data from the SWAT model with the corrected data from the ETA-HADGEM2-ES model were then evaluated in comparison with the current data in order to test the study hypothesis.

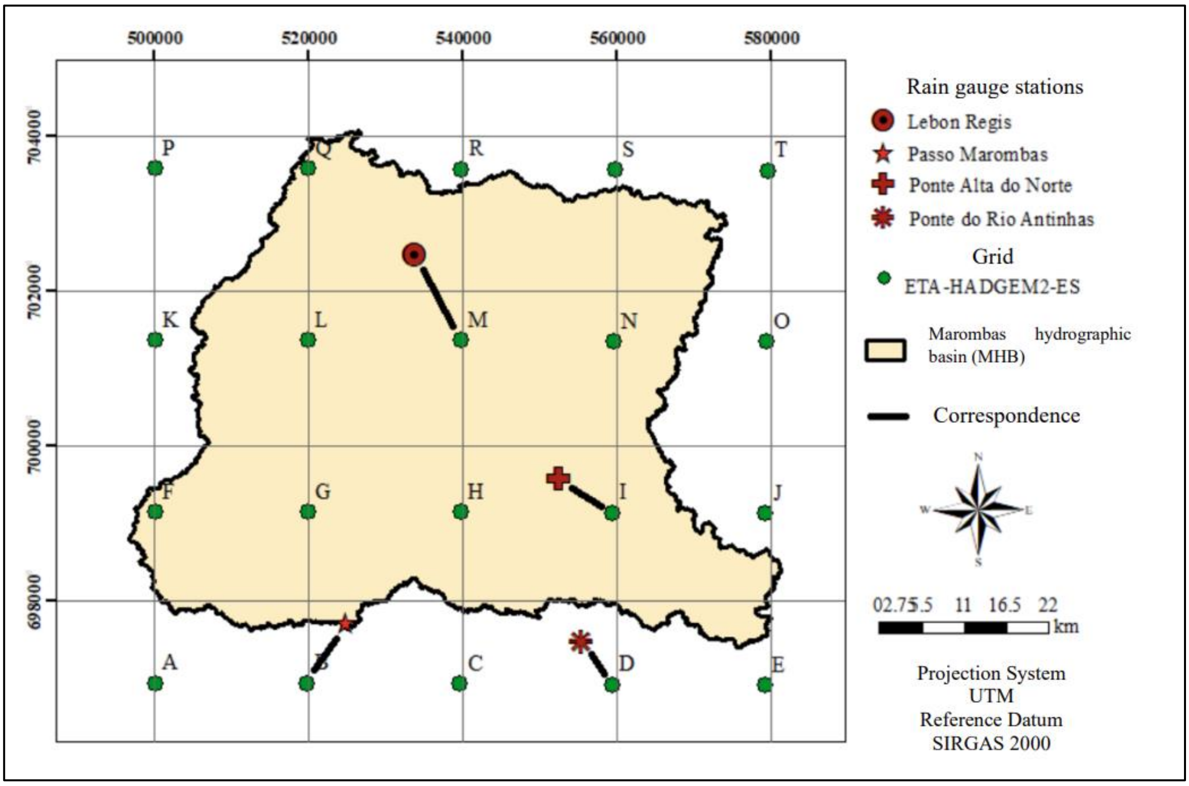

Figure 3. Correspondence between surface rainfall stations and grid points of the ETA-HADGEM2-ES model. Source: Author (2023).

Results and discussion

SWAT model calibrated and validated

The Nash-sutcliffe (NSE) values found were 0.91 for calibration and 0.74 for flow validation, which indicates a very good performance of the model in the modeling according to the classification of Santhi et al. (2001). According to this classification, the NSE values are stratified in relation to their performance in: very good (NSE≥0.65), good (0.65>NSE≥0.54) and satisfactory (0.54>NSE≥0.50). The result of sediment flow calibration was considered very good (NSE≥0.65) and the validation was satisfactory (0.54>NSE≥0.50).

These values are similar to those found in other studies in Brazil regarding the estimate of sediment production using the SWAT model. Paim and Menezes (2009) assessed the applicability of SWAT in the Tijucas River watershed, located on the coast of Santa Catarina, obtaining NSE values of 0.60, indicating a good fit of the model to the observed sediment data. Baltokoski et al. (2010) conducted a study involving SWAT and phosphorus loss in the Pinheiro and Conrado River micro-watersheds, achieving good NSE results, with values around 0.68. Pontes et al. (2021) evaluated the capacity of SWAT to simulate monthly flow and sediment load in the Posses stream watershed in southeastern Brazil, using the SUFI-2 algorithm for calibration and testing. The simulations achieved NSE values of 0.75 during calibration and 0.51 during testing for flow, and NSE values of 0.65 during calibration and 0.52 during testing for sediment load. In other parts of the world, good results have also been observed, such as in the work by Regasa and Nones (2023), who used SWAT to assess the impact of land use changes on erosion and sediment yield in the Fincha River watershed in Ethiopia. The model, calibrated and validated with data from 1986 to 2008, showed an NSE of 0.83 for runoff and 0.63 for sediments.

Validation of Climatic Data

The monthly data of maximum and minimum air temperature observed in the field and simulated by the model showed significant differences (α = 0.05). The model tended to underestimate the maximum temperature values in all months of the year. The minimum air temperature was also underestimated with maximum deviations of -5.3 in February. Relative humidity and solar radiation were also underestimated by the model, with maximum deviations of 12.8% and 108.4 MJ m² day^{-1}, respectively. In these cases, the projection data for the three variables showed significant differences ($\alpha = 0.05$) in relation to the observed data. The wind speed variable was overestimated by the model with a maximum deviation of 1.8 m s^{-1}. According to Chou et al (2014), in Brazil the ETA-HADGEM2-ES model underestimates the annual air temperature cycle for most of the year.

The precipitation data indicated that there were similar deviations in all evaluated seasons, with the largest variations occurring in the months of January, February and May. This greater deviation in the months of January and February may be related to the occurrence of more convective rains, which are more difficult to model due to spatial heterogeneity. In view of these differences, the data were submitted to correction using the Direct Approach method, as used by Moura (2020). According to Lenderink et al. (2007), the Direct Approach technique allows the direct use of outputs from regional climate models through some corrections that involve detecting differences between current climate conditions (observed at meteorological stations and simulated by the model) and applying these differences to the projected future series.

Effect of Climate Change Scenarios on Flow

The use of future climate change scenarios indicated an increase in the long-period average flow (Q_{MLP}) of 10.42% for the RCP 4.5 scenario and 16.42% for the RCP 8.5 scenario in relation to the base period (91.03 m³s-1). In Figure 4, the box plot graphs obtained for the base period and for the two scenarios used are presented.

It can be seen in Figure 4 that in addition to the increase observed in long-period average flows (QMLP), there is also greater temporal variability in flows as a result of the greater standard deviation obtained in the two hydrological scenarios. The magnitude of events also tends to increase, as the results indicated a greater occurrence of maximum events in the evaluated scenarios compared to the base period, as also verified by Moura (2020).

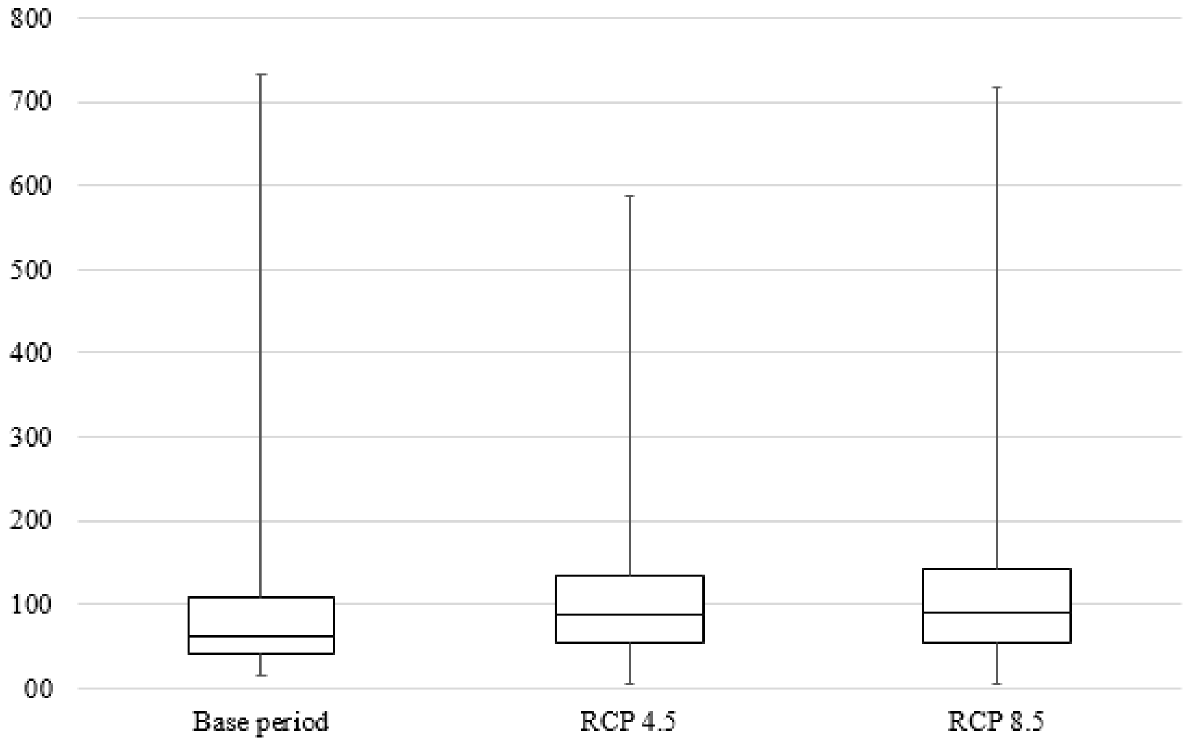

Figure 2. Boxplot of flows for the base period and for RCP 4.5 and RCP 8.5. Source: Author (2023).

In a monthly analysis of flows, there was a significant increase ($\alpha = 0.05$) in flows in the months of April and September for the two scenarios tested in relation to the base period (Figure 5). In the other months, no significant differences were found between the scenarios and the base period. However, it was possible to notice a tendency of increasing precipitation mainly between the months of September and December.

There is a shift in the highest average monthly flows from the month of July, in the base period, to the month of September. It must be considered, however, that the average monthly flow in July was overestimated due to the 1983 flood event, which assumed values well above the historical average.

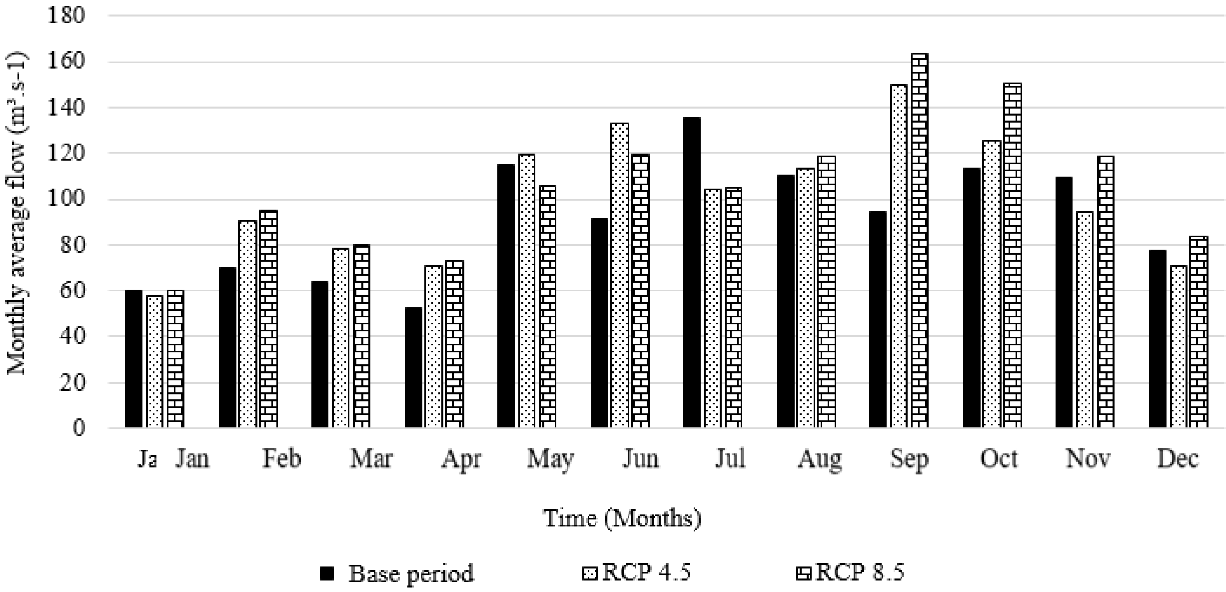

Figure 3. Comparison between monthly flow averages in the base period, RCP 4.5 and RCP 8.5 (2020-2099). Source: Author (2023).

Another way to evaluate the impact of changes in climate scenarios on flows is based on the permanence curve (Figure 6). This allows a visual assessment of how the two climate scenarios can influence the average daily flows in the study region. It can be seen that most of the time the RCP 4.5 and 8.5 scenarios presented flow values higher than the base period, with a drastic drop in the lowest flow values, a time when water availability is lower.

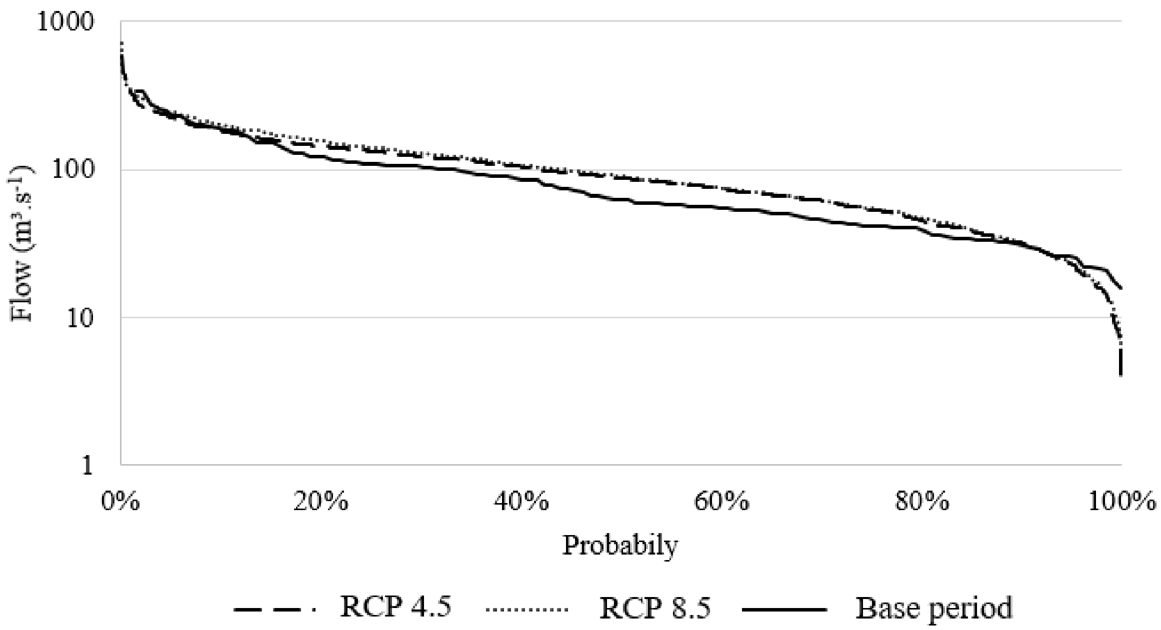

Figure 4. Flow persistence curve for the base period and for the two alternative climate change scenarios. Source: Author (2023).

Table 1 presents the reference flow values for the base period and for the two scenarios used. The Q50 reference flow increased by approximately 40% in the RCP 4.5 and RCP 8.5 scenarios. This can result in a higher average flow throughout the year, maintaining water availability in the region at levels suitable for urban and agricultural supply.

Table 1. Reference flows for the base period and for RCP 4.5 and 8.5 scenarios.

Flow Reference	Base Period	Reference Flow		Percentage of Change	
		RCP 4.5	RCP 8.5	RCP 4.5	RCP 8.5
	------------------ $m.s^{-1}$ ------------------			------------------ % ------------------	
Q_5	230.0	222.3	242.6	-3.3	5.5
Q_{10}	188.3	181.7	201.0	-3.5	6.7
Q_{50}	62.5	87.4	87.5	39.6	39.8
Q_{90}	30.9	31.4	31.8	1.8	3.1
Q_{95}	25.2	22.9	23.0	-11.5	-11.1
Q_{98}	21.1	15.5	15.4	-26.4	-27.1

Source: Author (2023).

The other reference flows used in granting water use Q_{95} and Q_{98} were reduced in the evaluated scenarios. Q_{95} showed a reduction of approximately 11% in both scenarios and Q98 had a decrease of 26.4% and 27.1% in the RCP 4.5 and RCP 8.5 scenarios, respectively. Considering this, it is suggested to continuously review the criteria for granting water use, taking into account possible future climate changes. The results of Q_{95} and Q_{98} indicate that in the future there may be a reduction in flow during the driest periods of the year. This indicates that although the model projects an increase in Q_{50}, the risk of more severe droughts in the region must be taken into account.

The reference flows Q_{10} and Q_5, which represent the maximum flows, showed a reduction of 3.5% in the RCP 4.5 scenario and an increase of 5.5% for Q_5 and 6.7 for Q_{10} in the RCP 8.5 scenario. This demonstrates a reduction in rainfall with greater volume in the RCP 4.5 scenario and an increase in this rainfall for the RCP 8.5 scenario, which projects an increase in temperature. However, as the data are daily, the model, in the structure used in this work, does not allow assessments in terms of rainfall intensity. For the study of maximum flows and sediment production, rainfall intensity is fundamental, as it is used to calculate peak flow and also to define rainfall erosivity.

Effect of Climate Change Scenarios on Sediment Flow

The average monthly sediment flow observed in the base period and projected for scenarios RCP 4.5 and 8.5 demonstrates that there was a considerable increase in their values in the two scenarios analyzed (Figure 7). In annual terms, the projections indicated that the flow of sediments tends to show an increase of 351% in RCP 4.5 and 368% in RCP 8.5.

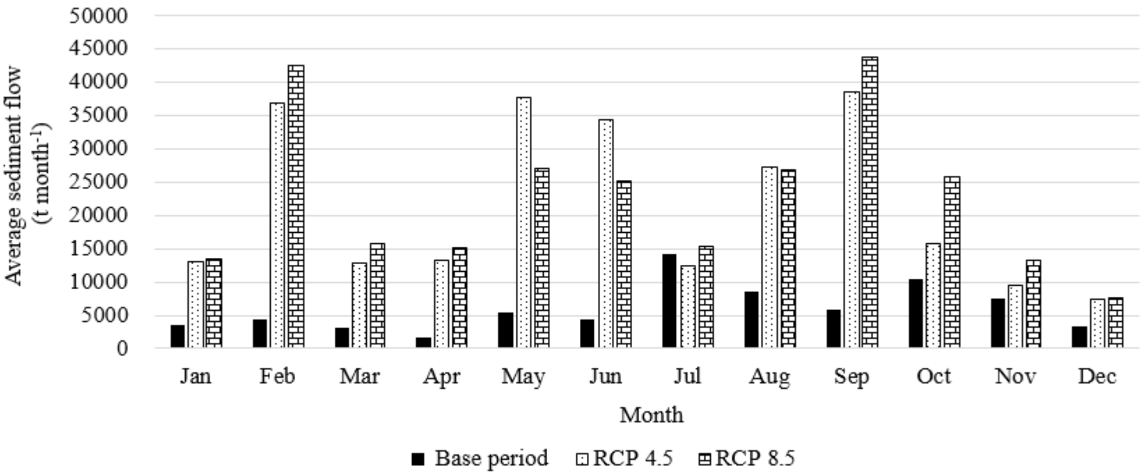

Figure 7. Comparison between monthly flow averages in the base period, RCP 4.5 and RCP 8.5 (2020-2099). Source: Author (2024)

The months of February, April, May, June and September showed the greatest intensification of water erosion in both scenarios (Table 2). In these months there was also a considerable increase in the volume of rain, as can be seen in Table 2. The volume of rain is one of the main characteristics that regulates the process of water erosion. Thus, the greater the volume of rain, the greater the volume of runoff and, consequently, the greater the water erosion (Ballabio et al., 2017). Therefore, it is expected that, with climate change, the precipitated volume will increase and, with this, the sediment flow will also increase, as indicated by the data simulated in this work.

Table 2. Average monthly sediment flow and average monthly rainfall in the base period and in the two climatic scenarios analyzed.

Month	Sediments flow			Alteration		Increase of monthly ranfall	
	Base period	RCP 4.5	RCP 8.5	RCP 4.5	RCP 8.5	RCP 4.5	RCP 8.5
	------------t $month^{-1}$------------			----------------------%----------------------			
January	3625	12994	13503	258	272	-6	-12
February	4328	36864	42460	752	881	18	20
March	3163	12844	15783	306	399	15	16
April	1754	13209	15185	653	766	14	22
May	5495	37703	27034	586	392	46	35
June	4328	34389	25210	695	482	30	29
July	14213	12404	15390	-13	8	0	7
August	8586	27325	26856	218	213	8	13
September	5804	38414	43757	562	654	31	47
October	10479	15752	25680	50	145	9	27
November	7570	9547	13304	26	76	15	30
December	3409	7388	7684	117	125	8	12

Source: Author (2023).

In the months of January, August, October, November and December there was an increase in the average monthly rainfall, however, to a lesser extent than in the other months (Table 3). As expected, the modeling result indicated that this reflects less intensification of the erosion process, resulting in less sediment flow in the basin's exudatory. The month of July had the least effect of using climate change scenarios on sediment production. It should be taken into account, however, that in July the average monthly sediment flow was greater due to the effect of a critical event that occurred in 1983. This event drove the average upwards, reducing the relative differences between the projected and observed value. Although the increase in sediment production was expected in a scenario of increased rainfall, the changes were very high, reaching almost 900% in February in RCP 8.5. This possible overestimation of the projections is partly the result of the model's weakness in its ability to calibrate and validate. The SWAT model tended to overestimate the flows, mainly during the validation period, potentially resulting from the implementation of crops in the form of no-tillage (NT) to replace native vegetation in the region. This change in the land use condition was not represented in the model.

To test whether the overestimation in the calibration and validation of the sediment flow with the SWAT model was responsible for a possible overestimation of the projections, the data projected for the climate scenarios were compared with the average monthly flow estimated by the model (Figure 8 and Table 3). It can be seen that. using simulated data as a comparison, there is a reduction in the percentage of change in sediment flow in both scenarios. This indicates the veracity of the hypothesis that part of the possible overestimation of sediments is the result of errors arising from the calibration and validation of the model.

Table 3. Comparison between the average monthly sediment flow and the average monthly rainfall between the data simulated in the calibration and validation of the model and the two scenarios analyzed

Month	Sediments flow			Alteration		Increase of monthly ranfall	
	Simulated*	RCP 4.5	RCP 8.5	RCP 4.5	RCP 8.5	RCP 4.5	RCP 8.5
	------------t month^{-1}------------			-----------------------%-----------------------			
January	5157	12994	13503	152	162	-6	-12
February	7214	36864	42460	411	489	18	20
March	5579	12844	15783	130	183	15	16
April	3496	13209	15185	278	334	14	22
May	6952	37703	27034	442	289	46	35
June	6131	34389	25210	461	311	30	29
July	6995	12404	15390	77	120	0	7
August	6522	27325	26856	319	312	8	13
September	7474	38414	43757	414	485	31	47
October	11293	15752	25680	39	127	9	27
November	7883	9547	13304	21	69	15	30
December	5642	7388	7684	31	36	8	12

Source: Author (2023). *The average sediment flux was obtained from simulated data in the calibration (1977 to 1978) and validation (1994 to 1997) of the model.

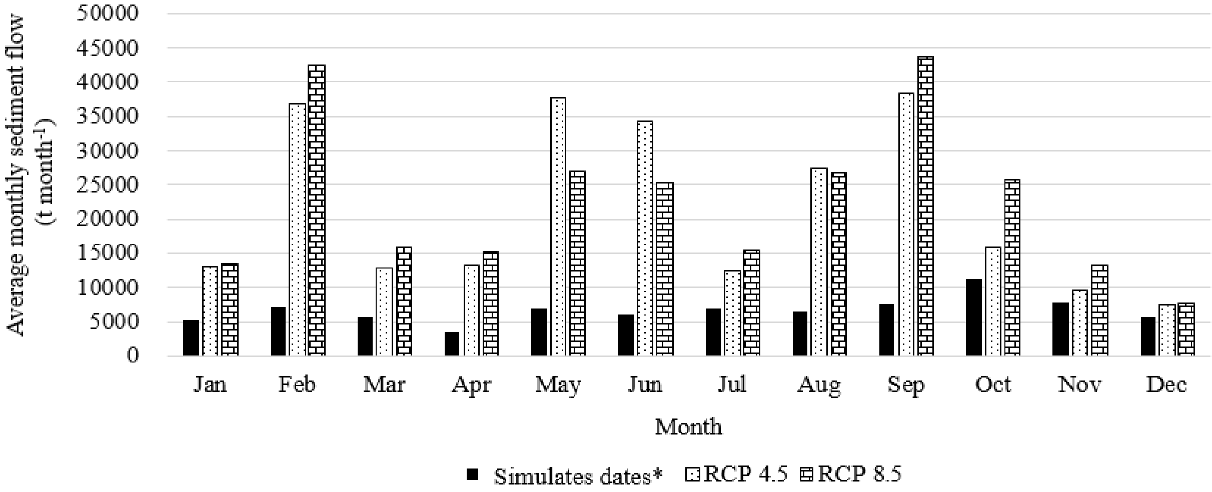

Figure 8. Comparison between monthly flow averages in the base period, RCP 4.5 and RCP 8.5 (2020-2099). Source: Author (2024)

Another factor that can be used to explain this high increase in sediment production in MHB is the temporal distribution of rainfall. Figure 9 presents a comparison of the number of days with rain in the month between the data measured at the rain gauge stations and the data projected by the model. The graphs demonstrate that, at all projected points and in all months, the number of days with rain increased.

The results in Figure 9 point out that in the projected scenarios, rainfall will occur in a better distributed manner over time, considerably altering the effects on water erosion, The SWAT model simulates the sediment production rate for each URH from the MUSLE equation. In this equation, the rain erosivity factor is replaced by runoff. This. in turn, is highly dependent on the soil's previous moisture. The occurrence of several rainy days in a row makes the soil maintain water content always close to its maximum water storage capacity. This makes even low-volume rains sufficient to generate high runoff. The practical experiences of monitoring sediment production demonstrate that the relationship between erosion and soil moisture is exponential, that is, the increase in the water content in the soil increases, more and more. the runoff and, consequently, the soil water erosion.

This change in climatic behavior, then, will cause the soil to remain with greater humidity, intensifying the erosion process. This would justify the results generated by the model projections, in which the increase in sediment production was higher than the increase in rainfall and flow

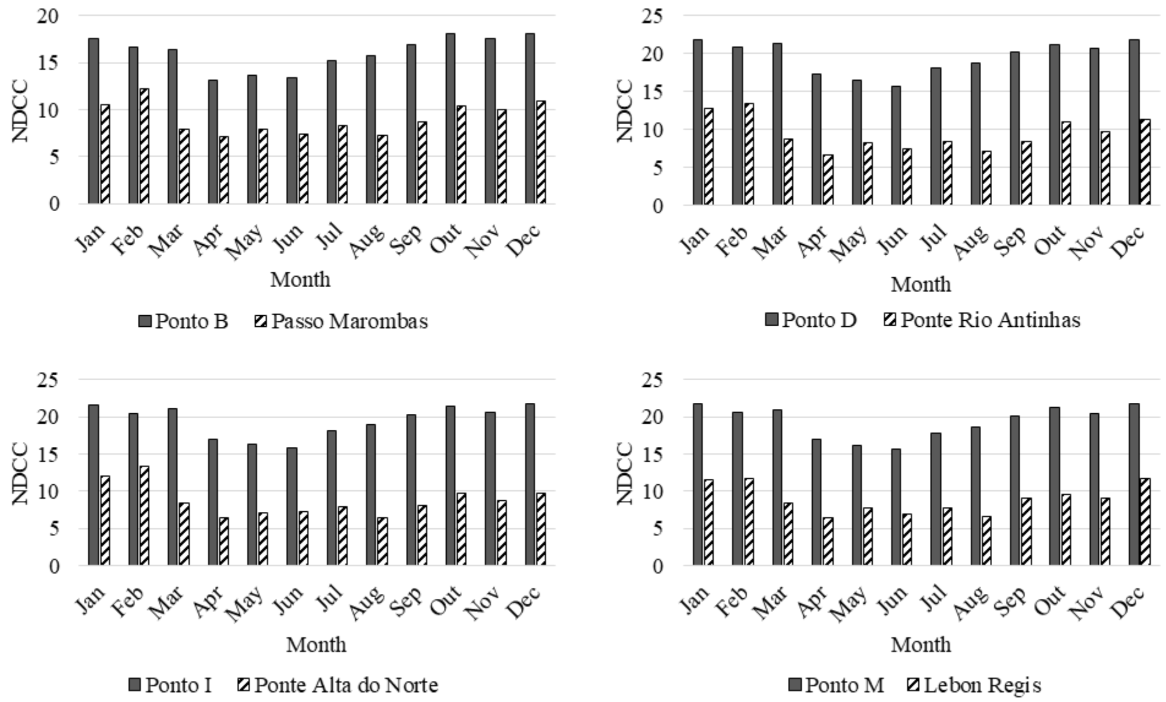

Figure 5. Comparison of the number of days with rain (NDWR) in the month between the data obtained in the pluviometric stations and projected in the scenario RCP 4.5. Source: Author (2023).

These results strengthen the hypothesis that the flow of sediments is greater when climate change results in increased rainfall with a better distributed pattern over time. In this condition, the RCP 8.5 scenario, which is more extreme, tends to present increases in the production of more severe sediments than the RCP 4.5 scenario, in the long run, as shown in Figure 10.

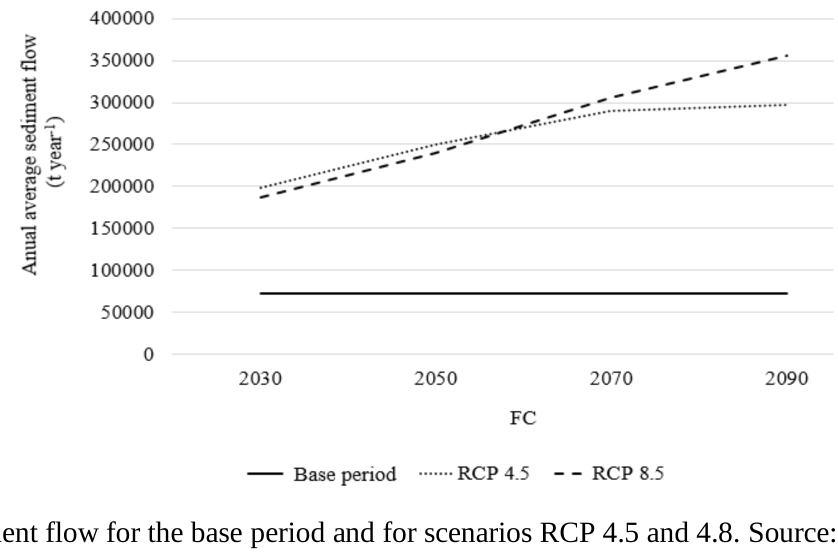

Figure 6. Sediment flow for the base period and for scenarios RCP 4.5 and 4.8. Source: Author (2023).

Conclusion

The SWAT model is suitable for estimating sediment flow and water flow in monthly terms, using climatic data projected by

ETAHADGEM2-ES. The model indicates that there is a tendency to increase the average water flow (Q_{50}) and reduce the basic water flow (Q_{95} and Q_{98}) in the two scenarios, RCP 4.5 and 8.5. This results in greater water availability for most of the year and less availability in times of drought. The sediments flow is altered as a result of climate change. The monthly values will be about three times higher in the future compared to the historical average used for calibration and validation of the SWAT model. The increase in the sediments flow is mainly due to the increase in the volume of rain and the fact that the rains become better distributed over time. The better temporal distribution of rain causes the soil moisture to remain closer to its maximum water storage capacity through the soil, influencing the runoff even with low rain volumes. The runoff, in turn, is the main agent in the transport of sediments, explaining the increase in soil water erosion.

Aknowledgements

This study was supported by the Soil Use and Conservation Laboratoryof the State University of Santa Catarina - UDESC and financed by the CAPES student scholarship program.

The authors thank the postgraduate program in Soil Sciences of the University of the State of Santa Catarina - UDESC and the Centro de Ciências Agroveterinarias - CAV/UDESC.

References

Amore, E., Modica, C., Nearing, M. A., Santoro, V. C., 2004. Scale effect in USLE and WEPP application for soil erosion computation from three Sicilian basins. Journal of Hydrology 293, 100-114. https://doi.org/10.1016/j.jhydrol.2004.01.018

Arnold, J. G., Moriasi, D., Gassman, P., Abbaspour, K. C., 2012. SWAT: Model use calibration and validation. Transactions of ASABE 55(4), 1494-1508. https://doi.org/10.13031/2013.42256

Baldissera, P., 2005. Aplicabilidade do modelo de simulação hidrológica SWAT (Soil And Water Assessment Tool), para a bacia hidrográfica do rio Cuiabá/MT. 142 p. Dissertação (Pós-graduação de Física e Meio Ambiente) – Universidade Federal de Mato Grosso. Cuiabá.

Ballabio, C., et al., 2017. Mapping monthly rainfall erosivity in Europe. Science of The Total Environment 579, https://doi.org/10.1016/j.scitotenv.2016.11.123

Baltokoski, V., Tavares, M. H. F., Machado, R. E., Oliveira, M. P., 2010. Calibração de modelo para a simulação de vazão e de fósforo total nas sub-bacias dos rios Conrado e Pinheiro – Pato Branco (PR). Revista Brasileira de Ciências do Solo 34, 253-261. https://doi.org/10.1590/S0100-06832010000100026

Barry, R. G., Chorley, R. J., 2013. Atmosfera, tempo e clima. Porto Alegre: Editora Bookman.

Bittencourt, D. P., Fuentes, M. V., Franke, A. E., Silveira, R. B., Alves, M. P. A., 2020. The climatology of cold and heat waves in Brazil from 1961 to 2016. International Journal of Climatology 40(4), 2464-2478. 10.1002/joc.6345

Breslow, P. B., Sailor, D. J., 2002. Vulnerability of Wind Power Resources to Climate Change in the Continental United States. Renewable Energy 27(4), 585-598. https://doi.org/10.1016/S0960-1481(01)00110-0

Chou, S. C., Lyra, A., Mourão, C., Dereczynski, C. P., 2014. Evaluation of the Eta Simulations Nested in Three Global Climate Models. American Journal of Climate Change 3(5), 438–454. https://doi.org/10.4236/ajcc.2014.35039

Ciais, Ph., Reichstein, M., Viovy, N., Granier, A., Ogée, J., Allard, V., Aubinet, M., Buchmann, N., Bernhofer, Chr., Carrara, A., Chevallier, F., De Noblet, N., Friend, A. D., Friedlingstein, P., Grünwald, T., Heinesch, B., Keronen, P., Knohl, A., Krinner, G., Loustau, D., Manca, G., Matteucci, G., Miglietta, F., Ourcival, J. M., Papale, D., Pilegaard, K., Rambal, S., Seufert, G., Soussana, J. F., Sanz, M. J., Schulze, E. D., Vesala, T., Valentini, R., 2003. Europe-wide reduction in primary productivity caused by the heat and drought in 2003. Nature 437(7058), 529–533. https://doi.org/10.1038/nature03972

De Moura, C. N., Rafaeli Neto, S. L., Campos, C. C. G., & Sá, E. A. S. (2020). Hydrological impacts of climate change in a well-preserved upland watershed. Water Resources Management, 34, 2255–2267. https://doi.org/10.1007/s11269-019-02450-1

Empresa Brasileira de Pesquisa Agropecuária, 2004. Levantamento de reconhecimento dos solos do Estado de Santa Catarina. Rio de Janeiro: Embrapa Solos. Mapa. Escala 1:250.000.

Escobar, E., Carvalho-Santos, C., 2022. Impacts of future climate on water ecosystem services in the watershed of the river Homem (northwest

Portugal). Finisterra, Lisboa, n. 120, p. 109-128, ago. 2022. https://doi.org/10.18055/finis26254

Filgueras, A. S., Silva da Silva, T., Stalliviere Corrêa, I. C., 2024. Impactos do aumento do nível do mar e ocupação do solo sobre zonas úmidas costeiras: Metodologia aplicada à Baía da Babitonga (SC). Sociedade Natural 36, 2024. https://doi.org/10.14393/SN-v36-2024-69403.

Filonchyk, M., Peterson, M., Zhang, L., Hurynovich, V., & He, Y. (2024). Greenhouse gases emissions and global climate change: Examining the influence of CO2, CH4, and N2O. The Science of the Total Environment, 935(2), 173359. https://doi.org/10.1016/j.scitotenv.2024.173359

Fox, J., 2008. Applied regression analysis and generalized linear models. Sage.

Groissman, P., et al., 2005. Trends in intense precipitation in the climate record. Journal of Climate 18, p. 1326-1350. Disponível em: https://journals.ametsoc.org/doi/10.1175/JCLI3339.1

Groppo, J. D., Moraes, J. M., Beduschi, C. E., Martinelli, L. A., 2005. Análise de séries temporais de vazão e precipitação em algumas bacias do Estado de São Paulo com diferentes graus de intervenções antrópicas. Geociências 24(2), 181-193.

Harrison, G. P., Cradden, L. C., Chick, J. P., 2008. Preliminary assessment of climate change on the UK onshore wind energy resource. Energy Sources 30(14), 1286-1299.

IPCC, 2007. Summary for policymakers. In: Parry, M. L., et al. (Ed.), Climate change 2007: impacts, adaptation and vulnerability; contribution of the Working Group II to the Fourth Assessment Report of the Intergovernmental Panel on Climate Change.

IPCC, 2013. The physical science basis. In: Climate change 2013: Working group I contribution to the fifth assessment report of the Intergovernmental Panel on Climate Change. Intergovernmental Panel on Climate Change, Geneva.

IPCC, 2023. Summary for Policymakers. In: P.R. Shukla, J. Skea, R. Slade, A. Al Khourdajie, R. van Diemen, D. McCollum, M. Pathak, S. Some, P. Vyas, R. Fradera, M. Belkacemi, A. Hasija, G. Lisboa, S. Luz, J. Malley, (Eds.), Climate Change 2023: Impacts, Adaptation, and Vulnerability. Contribution of Working Group II to the Sixth Assessment Report of the Intergovernmental Panel on Climate Change. Cambridge University Press, Cambridge, UK and New York, NY, USA.

Kalkhoff, S. J., Hubbard, L. E., Tomer, M. D., James, D. E., 2016. Effect of variable annual precipitation and nutrient input on nitrogen and phosphorus transport from two Midwestern agricultural watersheds. Sci. Total Environ. 543-562. https://doi.org/10.1016/j.scitotenv.2016.03.127

Koehler, H. S., Watzlawick, L. F., Kirchner, F. F., 2002. Fontes e níveis de erros nas estimativas do potencial de fixação de carbono. In: Sanquetta, C. R., Watzlawick, L. F., Balbinot, R. (Eds.), As florestas e o carbono. Curitiba: FUPEF/Imprensa da UFPR, 251-264.

Le Quéré, C., Moriarty, R., Andrew, R. M., Canadell, J. G., Sitch, S., Korsbakken, J. I., Friedlingstein, P., Peters, G. P., Andres, R. J., Boden, T. A., Houghton, R. A., House, J. I., Keeling, R. F., Tans, P., Arneth, A., Bakker, D. C. E., Barbero, L., Bopp, L., Chang, J., Chevallier, F., Chini, L. P., Ciais, P., Fader, M., Feely, R. A., Gkritzalis, T., Harris, I., Hauck, J., Ilyina, T., Jain, A. K., Kato, E., Kitidis, V., Klein Goldewijk, K., Koven, C., Landschützer, P., Lauvset, S. K., Lefèvre, N., Lenton, A., Lima, I. D., Metzl, N., Millero, F., Munro, D. R., Murata, A., Nabel, J. E. M. S., Nakaoka, S., Nojiri, Y., O'Brien, K., Olsen, A., Ono, T., Pérez, F. F., Pfeil, B., Pierrot, D., Poulter, B., Rehder, G., Rödenbeck, C., Saito, S., Schuster, U., Schwinger, J., Séférian, R., Steinhoff, T., Stocker, B. D., Sutton, A. J., Takahashi, T., Tilbrook, B., van der Laan-Luijkx, I. T., van der Werf, G. R., van Heuven, S., Vandemark, D., Viovy, N., Wiltshire, A., Zaehle, S., Zeng, N., 2015. Global carbon budget. Earth System Science Data 7(1), 47-85.

Lelis, T. A., Calijuri, M. L., Fonseca, A. S., Lima, D. C., 2011. Impactos causados pelas mudanças climáticas nos processos erosivos de uma bacia hidrográfica: Simulação de cenários. Revista Ambiente & Água 6(2). https://doi.org/10.4136/ambi-agua.200.

Lenderink, G., Buishand, A., & van Deursen, W. (2007). Estimates of future discharges of the river Rhine using two scenario methodologies: direct versus delta approach. Hydrology and Earth System Sciences, 11(3), 1145–1159. https://doi.org/10.5194/hess-11-1145-2007

Lensen, I., Schultz, G. B., Santos, I. (2015). Simulação dos impactos hidrossedimentológicos causados pelas mudanças climáticas na bacia hidrográfica do rio Apucaraninha, sul do Brasil. Proc. IAHS, 367, 366–373, https://doi.org/10.5194/piahs-367-366-2015.

Lovino, M. A., Muller, G. V., Sgroi, L. C., 2020. ¿Cómo ha cambiado la precipitación en la provincia de Santa Fe? RIA. Rev. Investig. Agropecu., Ciudad Autónoma de Buenos Aires, 46(2), 226-239.

Machado, R. L., Carvalho, D. F., Costa, J. R., Oliveira Neto, D. H., Pinto, M. F., 2008. Análise da erosividade das chuvas associada aos padrões de precipitação pluvial na região de Ribeirão das Lajes (RJ). Revista Brasileira de Ciência do Solo 32, 2113-1223. https://doi.org/10.1590/S0100-06832008000500032.

Marengo, J. A., 2006. Mudanças climáticas globais e seus efeitos sobre a biodiversidade: caracterização do clima atual e definição das alterações climáticas para o território brasileiro ao longo do século XXI. Biodiversidade 26.

Mazurczyk, T., Piekielek, N., Tansey, E., Goldman, B., 2018. American archiver and climate change: Risk and adaptation. Climate Risk Management 20, 111-125. https://doi.org/10.1016/j.crm.2018.03.005.

McKay, N. P., Overpeck, J. T., Otto-Bliesner, B. L., 2011. The role of ocean thermal expansion in Last Interglacial sea level rise. Geophysical Research Letters 38(14). https://doi.org/10.1029/2011GL048280.

Moser, D. E., Thomas, E. R., Nehrbass-Ahles, C., Eichler, A., Wolff, E. Review article: Melt-affected ice cores for polar research in a warming world. The Cryosphere 18(6):2691-2718. https://doi.org/10.5194/tc-18-2691-2024.

Oliveira, G. G., Pedrollo, O. C., Castro, N. M. R., 2015. Stochastic approach to analyzing the uncertainties and possible changes in the availability of water in the future based on scenarios of climate change. Hydrology and Earth System Sciences 19(8), 3585–3604. https://doi.org/10.5194/hess-19-3585-2015.

Paim, J. B., Menezes, J. T., 2009. Estimativa do balanço sedimentar da bacia do rio Tijucas (SC-Brasil) a partir da aplicação do modelo hidrológico SWAT. Revista Geográfica Acadêmica 3(2), 5-14.

Poelking, E. L., Andrade, A. M., Vieira, G. B. T. G., & Schaefer, C. E. G. R. (2014). Variações da frente da geleira polar Club, península Potter (Ilha Rei George, Antártica marítima) entre 1986 e 2011. Revista Brasileira de Meteorologia, 29(3), 379–388. https://doi.org/10.1590/0102-778620120439

Pontes, L. M., Batista, P., Silva, B. P. C., Viola, M. R., Rocha, H., Silva, M. L. N. (2021). Avaliação da produção de sedimentos e vazão com modelo SWAT em uma pequena sub-bacia do Sistema Cantareira. Revista Brasileira de Ciências do Solo. 45. https://doi.org/10.36783/18069657rbcs20200140.

Regasa M. S, Nones, M. (2023). SWAT model-based quantification of the impact of land use land cover change on sediment yield in the Fincha watershed, Ethiopia. Front. Environ. Sci., 11. https://doi.org/10.3389/fenvs.2023.1146346

Royston, P. (1982). An extension of Shapiro and Wilk's W test for normality to large samples. Applied Statistics, 115–124.

Salviano, M. F., Groppo, J. D., & Pellegrino, G. Q. (2016). Análise de tendências em dados de precipitação e temperatura no Brasil. Revista Brasileira de Meteorologia, 31(1), 64-73. Disponível em: http://www.scielo.br/pdf/rbmet/v31n1/0102-7786-rbmet-31-01-0064.pdf. Acesso em: 31 jan. 2019.

Santhi, C. J. G., Arnold, J. G., Williams, J. R., Dugas, W. A., Srinivasan, R., & Hauck, L. M. (2001). Validation of the SWAT Model on a large River Basin with point and Nonpoint Sources. Journal of the American Water Resource Association, 27(5), 1169-1188. https://doi.org/10.1111/j.1752-1688.2001.tb03630.x

Sartori, A., Genovez, A. M., & Lombardi Neto, F. (2005). Classificação hidrológica de solos brasileiros para a estimativa da chuva excedente com o método do serviço de conservação do solo dos Estados Unidos Parte 2: Aplicação. Revista Brasileira de Recursos Hídricos, 10(4). Disponível em: https://abrh.s3.sa-east-1.amazonaws.com/Sumarios/26/2ad1ccf5cc715b1182f18ada4b78a527_94e5e2ff168aa7bdb82e9438b8838466.pdf. Acesso em: 07 jan. 2019.

Schär, C., Vidale, P. L., Lüthi, D., Frei, C., Häberli, C., Liniger, M. A., & Appenzeller, C. (2004). The role of increasing temperature variability in European summer. Nature, 427, 332–336. https://doi.org/10.1038/nature02300.

Seebocus, R. H., Lollchund, M. R., & Bessafi, M. (2021). Analysis of extreme rainfall and drought events using statistical and fractal methods: A case study of Mauritius. S. Afr. J. Sci., Pretoria, 117(9-10), 1-9. Available from http://www.scielo.org.za/scielo.php?script=sci_arttext&pid=S0038-

23532021000500019&lng=en&nrm=iso. Access on 17 Sept. 2024. http://dx.doi.org/10.17159/sajs.2021/7477.

Shui, F., Zongpeng, C., Yang, Q., Hou, Y.,Wang, Z., Liu, F., Wang, B., Wang, W. (2024). Long-term changes of wind resources and its impact on wind power development under climate change in China. Energy Internet, v.1, 52-62. https://doi.org/10.1049/ein2.12001.

Tan, M. G., Gassman, P. W., Yang, X., & Haywood, J. (2020). A review of SWAT applications, performance and future needs for simulation of hydro-climatic extremes. Advances in Water Resources, 143, 103662. https://doi.org/10.1016/j.advwatres.2020.103662

Yang, J., Reichert, P., Abbaspour, K. C., Xia, J., & Yang, H. (2008). Comparing uncertainty analysis techniques for a SWAT application to the Chaohe Basin in China. Journal of Hydrology, 358(3-4), 119-130. https://doi.org/10.1016/j.jhydrol.2008.06.026

Wang, G., Du, B., Zhang, L., Jiang, H., & Xu, Z. (2014). Role of soil erodibility in affecting available nitrogen and phosphorus losses under simulated rainfall. Journal of Hydrology, 514, 180-191. https://doi.org/10.1016/j.jhydrol.2014.04.028

Zhenmei, M., Kang, S., Zhang, L., Tong, L., & Su, X. (2008). Analysis of impacts of climate variability and human activity on streamflow for a river basin in arid region of northwest China. Journal of Hydrology, 352(3-4), 239-249. https://doi.org/10.1016/j.jhydrol.2007.12.022

Zou, Y.; Wang, Y.; He, Y.; Zhu, L.; Xue, S.; Liang, X.; Ye, C (2024). Características da erosão do solo em bacias hidrográficas de ilhas tropicais com base sobre o modelo CSLE: Discussão sobre mecanismo. Land, 13, 302. https://doi.org/10.3390/land13030302